Emergence of helical edge conduction in graphene at the $\nu = 0$ quantum Hall state

Pavel Tikhonov,[1] Efrat Shimshoni,[1] H. A. Fertig,[2] and Ganpathy Murthy[3]

[1]*Department of Physics, Bar-Ilan University, Ramat-Gan 52900, Israel*
[2]*Department of Physics, Indiana University, Bloomington, IN 47405, USA*
[3]*Department of Physics and Astronomy, University of Kentucky, Lexington KY 40506-0055, USA*

(Dated: July 29, 2021)

The conductance of graphene subject to a strong, tilted magnetic field exhibits a dramatic change from insulating to conducting behavior with tilt-angle, regarded as evidence for the transition from a canted antiferromagnetic (CAF) to a ferromagnetic (FM) $\nu = 0$ quantum Hall state. We develop a theory for the electric transport in this system based on the spin-charge connection, whereby the evolution in the nature of collective spin excitations is reflected in the charge-carrying modes. To this end, we derive an effective field theoretical description of the low-energy excitations, associated with quantum fluctuations of the spin-valley domain wall ground-state configuration which characterizes the two-dimensional (2D) system with an edge. This analysis yields a model describing a one-dimensional charged edge mode coupled to charge-neutral spin-wave excitations in the 2D bulk. Focusing particularly on the FM phase, naively expected to exhibit perfect conductance, we study a mechanism whereby the coupling to these bulk excitations assists in generating back-scattering. Our theory yields the conductance as a function of temperature and the Zeeman energy - the parameter that tunes the transition between the FM and CAF phases - with behavior in qualitative agreement with experiment.

I. INTRODUCTION AND PRINCIPAL RESULTS

One of the most intriguing manifestations of many-body effects in graphene is the observation of a quantum Hall (QH) state at $\nu = 0$ in the presence of strong perpendicular magnetic fields[1–14]. This unique state is characterized by a plateau at $\sigma_{xy} = 0$, and a peak in the longitudinal resistance which typically exhibits insulating behavior. The high resistance signature is difficult to reconcile with a non-interacting theory[15], which implies a helical nature of the edge states: right and left movers have opposite spin flavors, resolved by the Zeeman splitting of the $n = 0$ Landau level in the bulk. In analogy with the quantum spin Hall (QSH) state in two-dimensional (2D) topological insulators[16,17], the edge states are hence immune to backscattering by static impurities, and a nearly perfect conduction is expected.

Coulomb interactions do not change the character of the edge states in a fundamental way, as long as the many-body state forming in the bulk remains spin-polarized, i.e. is a ferromagnet (FM). Such a bulk phase supports a gapless collective edge mode associated with a domain wall in the spin configuration, which can be modeled as a helical Luttinger liquid[18–21]. Insulating behavior therefore suggests that the true ground state is not a FM. Indeed, at half filling of the $n = 0$ Landau level, there is a rich variety of ways to spontaneously break the $SU(4)$ symmetry in spin and valley space, leading to a multitude of possible ground states with distinct properties[22–30]. The combined effect of interactions and external fields can assist in selecting the favored many-body ground state, particularly when accounting for lattice-scale interactions which do not obey $SU(4)$ symmetry. Most interestingly, the tuning of an external parameter can drive a transition from one phase to another. As a concrete example, it has been proposed[25,26,31] that a phase transition can occur from a canted antiferromagnetic (CAF) to a FM state, tuned by increasing the Zeeman energy E_z to appreciable values.

Recent experiments in a tilted magnetic field[32,33] appear to confirm the predicted phase transition in a transport measurement. In these experiments, the perpendicular field $B_\perp$ is kept fixed while the Zeeman coupling E_z is tuned by changing the parallel component. At $\nu = 0$ and relatively low E_z, the system exhibits a vanishing two-terminal conductance which slightly increases to finite values with increasing temperature T; i.e., it indicates an insulating behavior as in earlier studies of the $\nu = 0$ state. However with increasing values of E_z, the sample develops a steep rise of conductance and approaches an almost perfect two-terminal conductance of $G \approx 2e^2/h$, a behavior characteristic of a QSH state with protected edge states.

The most natural interpretation of these findings is in terms of the predicted phase transition from a CAF to a FM bulk state. However, while the theory dictates a second order quantum phase transition at a critical Zeeman coupling E_z^c (and $T = 0$), the transport data (obtained at finite T) reflects a smooth evolution of G with E_z. The critical point E_z^c can be estimated only roughly by, e.g., identifying the value of E_z where $G(T \to 0)$ approaches the mid-value e^2/h, or where dG/dT changes sign. At the highest accessible E_z (where presumably $E_z > E_z^c$), the conductance still falls below the perfect quantized value.

The above described behavior suggests that the low energy charge-carrying excitations smoothly evolve through the CAF-FM phase transition, so that their change of character reflects the critical properties of the bulk phases. In earlier work[34,35], we showed that in both phases one can construct collective charged modes associated with textures in the spin and valley configurations

near the edges of the system, and characterized their essential properties. Such excitations are supported due to the formation of a domain wall (DW) structure, where the spin and valley are entangled and vary with position towards the edge. The nature of collective edge modes continuously evolves as E_z is tuned through the transition. In particular, the CAF phase supports a gapped charged edge mode, which becomes gapless at the transition to the FM phase and is smoothly connected to the helical edge mode characteristic of the QSH state.

In terms of the spin degree of freedom, the gapless charged collective edge mode in the FM phase corresponds to a 2π twist of the ground-state spin configuration in the XY-plane[18]. This spin twist is imposed upon the spatially-varying S_z associated with the DW, thus creating a spin texture (i.e. a Skyrmion stretched out along the entire edge), with an associated charge that is inherent to quantum Hall ferromagnets[36–38]. In contrast, the energy cost of generating such a spin texture in the CAF phase is infinite. A proper description of the lowest energy charged excitations in this phase therefore involves a coupling between topological structures at the edge and in the bulk[34], and yields a charge gap on the edge that encodes the *bulk* spin stiffness for rotations in the XY-plane.

In both the CAF and FM phases, the collective excitations also contain charge-neutral modes, and among them the low-energy ones are spin-waves in the bulk[35]. Their behavior across the transition is the opposite of the charged edge modes: in the CAF phase, where the charged edge excitations are gapped, a broken $U(1)$ symmetry in the bulk (associated with XY-like order parameter) implies a neutral, gapless Goldstone mode. In contrast, in the FM phase where the charged edge mode is gapless, the bulk spin-waves acquire a gap which grows with $(E_z - E_z^c)$. While the neutral modes do not contribute to electric transport as carriers, their coupling to the charged modes can play an important role in the scattering processes responsible for a finite resistance. Most prominently, in the FM phase where the helical edge modes are protected by conservation of the spin component S_z, the coupling to the bulk spin-waves is essential to relax this conservation, and therefore dominates the electric resistance at finite T.

In a previous work[35], three of the present authors carried out a detailed time-dependent Hartree-Fock (TDHF) analysis of the HF state of our first paper[34]. TDHF is similar in spirit to a spin-wave analysis, in that it diagonalizes the Hamiltonian in the Hilbert space of a single particle-hole excitation. However, for our present purpose of investigating the transport on the edge near the transition, we need to go beyond TDHF in several ways. Firstly, we need to include a coupling between the edge and bulk modes that allows the relaxation of the edge spin, which is otherwise a good quantum number. Secondly, we need to introduce disorder at the edge, which is extremely hard to do in TDHF. Thirdly, we would like the temperature-dependence of transport coefficients close to the transition to compare to experiments.

To accomplish these objectives, in this paper we will first derive a low-energy effective field-theoretic description of the coupled system of bulk and edge, which encodes the information on the nature of the collective modes as well as the symmetries of the problem (overall S_z conservation, including both bulk and edge). The parameters appearing in this effective theory have to be matched with the results of TDHF as well as physical constraints such as the fact that the stiffness is not singular at the transition. Since we focus on the low-energy sector, the theory contains the charge-carrying edge mode (gapless in the FM phase) and neutral spin-wave excitations of the bulk (gapped in the FM phase). Interestingly, some of the parameters of the effective theory do behave in a singular way as the transition in approached, reflecting a divergent length scale.

This effective theory contains all the ingredients we need to compute transport coefficients at low temperatures. The detailed TDHF calculation[35] shows that all other collective excitations are high in energy, and remain gapped through the transition. They will thus contribute, at best, to a finite renormalization of the parameters of the effective theory.

Focusing particularly on the FM phase, we study the mechanism whereby the coupling of the charged edge mode to the charge-neutral bulk excitations assists in generating back-scattering. Our theory yields the two-terminal conductance G as a function of T and the Zeeman energy E_z. The main results are summarized in Fig. 1, and Eq. (4.24) below which describes the intrinsic resistance (dictating the deviation of G from $2e^2/h$) as a scaling function of T and the critical energy scale $\Delta = E_z - E_z^c$. In the low T limit where $T \ll \Delta$, this yields a simple activation form [see Eq. (4.25)]. This behavior is dual to the exponentially small *conductance* expected in the insulating CAF phase. Our results are in qualitative agreement with experiment.

The paper is organized as follows. In Sec. II we detail the derivation of a 2D field theoretical model for the quantum fluctuations in the spin and valley configuration for a system with an edge potential. In Sec. III we study the normal modes of low energy collective excitations in the FM phase, and derive an effective Hamiltonian describing the 1D edge mode coupled to 2D bulk spin-waves. This section is supplemented by Appendix A, devoted to a derivation of the scaling of the model parameter when E_z approaches the critical value E_z^c. Based on the resulting effective model, in Sec. IV we evaluate the two-terminal conductance G as a function of T and E_z. Some further details of the calculation are included in Appendix B. Finally, our main results and some outlook are summarized in Sec. V.

II. MODEL FOR SPIN-VALLEY FLUCTUATIONS IN TWO-DIMENSIONS

We consider a ribbon of monolayer graphene in the $x-y$ plane, subject to a tilted magnetic field of magnitude B_T and perpendicular component $B_\perp$. These two distinct field scales independently determine the Zeeman energy $E_z \propto B_T$ and the magnetic length $\ell = \sqrt{\hbar c/eB_\perp}$. At zero doping, the $n=0$ Landau level is half-filled and we assume that mixing with other Landau levels can be neglected. In addition, for the time being we focus on an ideal system uniform in the $\hat{y}$-direction but of finite width in the $\hat{x}$-direction, so that single-electron states can be labeled by a guiding-center coordinate $X = \ell^2 k_y$ with k_y the momentum in the y-direction. Similarly to Ref. 34, the boundaries of the ribbon are accounted for by an edge potential $U(x)\hat{\tau}_x$ where $\hat{\tau}_x$ denotes a valley isospin operator, and $U(x)$ grows linearly over a length scale w, from zero in the bulk to a constant U_e on the edge. It is therefore convenient to represent electronic states in a basis of 4-spinors $|X\, s\, \tau\rangle$ where $s = \uparrow, \downarrow$ denotes the real spin index s_z, and $\tau = \pm$ are the eigenvalues of $\hat{\tau}_x$ corresponding to symmetric and antisymmetric combinations of valley states.

The microscopic Hamiltonian describing the system, projected into the above manifold of $n=0$ states, assumes the form[25,26,34]

$$H = \sum_X c^\dagger(X)[-E_z\sigma_z\tau_0 + U(X)\sigma_0\tau_x]c(X) + H_{int}\ , \tag{2.1}$$

$$H_{int} = \frac{\pi\ell^2}{L^2}\sum_{\alpha=0,x,y,z}\sum_{X_1,X_2,q} e^{-q^2\ell^2/2+iq(X_1-X_2)} g_\alpha :c^\dagger(X_1+\frac{q\ell^2}{2})\tau_\alpha c(X_1-\frac{q\ell^2}{2})c^\dagger(X_2-\frac{q\ell^2}{2})\tau_\alpha c(X_2+\frac{q\ell^2}{2}):,$$

where $c^\dagger(X), c(X)$ are creation and annihilation operators written as 4-spinors, $[c^\dagger(X) \equiv (c^\dagger_{K,\uparrow}(X), c^\dagger_{K,\downarrow}(X), c^\dagger_{K',\uparrow}(X), c^\dagger_{K',\downarrow}(X))]$, σ_α (τ_α) are the spin (isospin) Pauli matrices and σ_0, τ_0 are unit matrices, L is the system size and :: denotes normal ordering; g_α denote lattice-scale interaction parameters obeying $g_x = g_y \equiv g_{xy}$ and $g_z > -g_{xy} > 0$. The latter condition is required[25] to stabilize a CAF phase for small E_z. Finally, g_0 parametrizes an $SU(4)$ symmetric interaction which mimics the effect of Coulomb interactions, and dominates the spin-isospin stiffness.

As we have shown in Ref. 34, for arbitrary E_z and $U(X)$ the Hartree-Fock solution of the Hamiltonian Eq. (2.1) at 1/2-filling is a spin-valley entangled domain wall, characterized by two distinct canting angles $\psi_a(X)$, $\psi_b(X)$ which vary continuously as a function of X when approaching an edge. This corresponds to a Slater determinant with two (out of four possible) occupied states for each X:

$$|a_X\rangle = \cos\frac{\psi_a}{2}|X\uparrow +\rangle - e^{i\phi_a}\sin\frac{\psi_a}{2}|X\downarrow -\rangle, \tag{2.2}$$
$$|b_X\rangle = -\cos\frac{\psi_b}{2}|X\uparrow -\rangle + e^{i\phi_b}\sin\frac{\psi_b}{2}|X\downarrow +\rangle,$$

where the X-dependence of ψ_ν, ϕ_ν is implicit. The many-body state is therefore a hybridized spin-valley configuration, which may be represented in terms of two local spin-1/2 pseudospin fields $\mathbf{S}_a(X)$, $\mathbf{S}_b(X)$ encoded by the Euler angles $\psi_\nu \in [0,\pi]$, $\phi_\nu \in [0, 2\pi]$:

$$\mathbf{S}_\nu = \frac{1}{2}\left(\sin\psi_\nu\cos\phi_\nu, \sin\psi_\nu\sin\phi_\nu, \cos\psi_\nu\right), \tag{2.3}$$

where $\nu = a, b$. Note that in Ref. 34, our focus was on the derivation of the ground state and we had assumed trivial phase factors in Eq. (2.2): $\phi_a = \phi_b \equiv \phi = 0$. However, there is actually a manifold of degenerate ground states with an arbitrary global phase $\phi \neq 0$. This implies the existence of a gapless mode associated with a slowly varying twist of the angle ϕ, consistent with Ref. 35 as will be discussed in more detail below.

We now allow for fluctuations in the collective variables $\psi_\nu(\mathbf{r})$, $\phi_\nu(\mathbf{r})$ [where $\mathbf{r} = (x,y)$] which vary slowly in space with respect to the magnetic length ℓ. Assuming further that $g_0 \sim e^2/\ell$ and hence is much larger than the other interaction scales (for $\alpha = x,y,z$, $g_\alpha \sim e^2 a_0/\ell^2$ with a_0 the lattice spacing[25]), a semi-classical approximation yields an effective Hamiltonian of the form

$$H[\mathbf{S}_a(\mathbf{r}), \mathbf{S}_b(\mathbf{r})] = \sum_{\mathbf{r}}\left\{\frac{\rho_0}{2}\sum_{\alpha=x,y,z}\sum_{\nu=a,b}|\nabla S^\alpha_\nu|^2 + H_{loc}(\mathbf{r})\right\} \tag{2.4}$$

where $\rho_0 \propto g_0$ is the pseudospin-stiffness, and $H_{loc}(\mathbf{r})$ is a local term. The latter can be derived by evaluating the expectation value of the microscopic Hamiltonian Eq. (2.1) in a state of the form Eq. (2.2), with the label X replaced by $\mathbf{r}$. Defining a local projector

$$\mathcal{P}(\mathbf{r}) = |a_\mathbf{r}\rangle\langle a_\mathbf{r}| + |b_\mathbf{r}\rangle\langle b_\mathbf{r}|\ , \tag{2.5}$$

the local energy term can be expressed as

$$H_{loc}(\mathbf{r}) = \sum_{\alpha=x,y,z} g_\alpha\left\{(Tr[\mathcal{P}(\mathbf{r})\sigma_0\tau_\alpha])^2 - Tr[(\mathcal{P}(\mathbf{r})\sigma_0\tau_\alpha)^2]\right\}, \tag{2.6}$$

where Tr is the trace of a 4×4 matrix in the basis set by the 4 states $|\uparrow\pm\rangle$, $|\downarrow\pm\rangle$. Employing Eqs. (2.2) and (2.5), we obtain

$$\begin{aligned} H_{loc}(\mathbf{r}) &= -[E_z - U(x)]\cos\psi_a(\mathbf{r}) - [E_z + U(x)]\cos\psi_b(\mathbf{r}) \\ &- (g_z + 3g_{xy})\cos\psi_a(\mathbf{r})\cos\psi_b(\mathbf{r}) - (g_z - g_{xy})\sin\psi_a(\mathbf{r})\sin\psi_b(\mathbf{r})\cos[\phi_a(\mathbf{r}) - \phi_b(\mathbf{r})]\ . \end{aligned} \tag{2.7}$$

Note that since the physical parameters obey $g_z > 0$ and $g_{xy} < 0$, the coefficient of the last term is always negative. Indeed, this term arises from the ferromagnetic coupling between the a and b pseudospins in the XY plane, and tends to lock the relative planar angle $\phi_- = \phi_a - \phi_b$ to $\phi_- = 0$. In contrast, H_{loc} does not contain any explicit dependence on the symmetric combination $\phi_+ = \phi_a + \phi_b$, signifying the gapless nature of its fluctuations.

Inserting Eq. (2.7) with $\phi_- = 0$ into Eq. (2.4), and minimizing $H[\mathbf{S}_a(\mathbf{r}), \mathbf{S}_b(\mathbf{r})]$ with respect to the remaining collective fields $\psi_a(\mathbf{r})$ and $\psi_b(\mathbf{r})$, yields the static domain wall structure $\psi_a^0(\mathbf{r}), \psi_b^0(\mathbf{r})$ described in Ref. 34: in the bulk, $\psi_a^0 = \psi_b^0 = \psi$ where in the CAF phase ($E_z < E_z^c = 2|g_{xy}|$) ψ is a nontrivial canting angle[25] obeying $\cos\psi = E_z/E_z^c$, and in the FM phase ($E_z > E_z^c$) $\psi = 0$; the angles smoothly change towards the edge where $\psi_a^0 = -\pi$, $\psi_b^0 = 0$ in both phases. Close to the CAF/FM transition ($E_z \to E_z^c$), the effective width of the domain wall is given by the diverging length scale

$$\xi \sim \sqrt{\rho_0/|E_z - E_z^c|}\ . \tag{2.8}$$

To describe the dynamics of *quantum* fluctuations in the collective pseudospin fields compared to their ground state configuration, we next construct a path-integral formulation[39] in terms of the Euclidean action

$$\mathcal{S}_{2D} = \int_0^\beta d\tau \left\{ -\frac{i}{2}\sum_{\mathbf{r}}\sum_{\nu=a,b}\cos\psi_\nu \partial_\tau \phi_\nu + H[\mathbf{S}_a, \mathbf{S}_b] \right\}, \tag{2.9}$$

where $\beta = 1/T$, $H[\mathbf{S}_a, \mathbf{S}_b]$ is given by Eq. (2.4), and the local fields are now $\psi_\nu(\mathbf{r},\tau)$, $\phi_\nu(\mathbf{r},\tau)$ with τ the imaginary time; here we have used units where $\hbar = k_B = 1$. Defining the fluctuation fields $\Pi_\nu(\mathbf{r},\tau)$ via the substitution

$$\cos\psi_\nu = \cos\psi_\nu^0 + \Pi_\nu \tag{2.10}$$

in the first term of Eq. (2.9), it is apparent that Π_ν are the canonical momenta of the planar angle fields ϕ_ν. Employing the canonical transformation into symmetric and antisymmetric fields

$$\begin{aligned} \phi_+ &= \frac{1}{2}(\phi_a + \phi_b)\ , \quad \phi_- = \phi_a - \phi_b, \\ \Pi_+ &= \Pi_a + \Pi_b\ , \quad \Pi_- = \frac{1}{2}(\Pi_a - \Pi_b)\ , \end{aligned} \tag{2.11}$$

the effective action acquires the form

$$\mathcal{S}_{2D} = \int_0^\beta d\tau \left\{ -\frac{i}{2}\sum_{\mathbf{r}}\sum_{\mu=+,-}\Pi_\mu \partial_\tau \phi_\mu + H[\Pi_+, \Pi_-, \phi_+, \phi_-] \right\}, \tag{2.12}$$

where in the last term, the dependence on ϕ_+ is restricted to gradient terms, while the ϕ_--dependence includes a mass term [the last term in Eq. (2.7), $\propto \cos\phi_-$] independent of E_z. As a result, the normal modes of the antisymmetric sector are typically gapped, and a low-energy effective field-theory model can obtained by projecting to the symmetric sector encoded by the pair of conjugate fields ϕ_+, Π_+. We note that the local momentum operator Π_+, denoting a fluctuation in the total spin component S_z,

$$\Pi_+ = \delta S_a^z + \delta S_b^z = \delta S^z\ , \tag{2.13}$$

commutes with all the local terms of $H[\Pi_+, \Pi_-, \phi_+, \phi_-]$. As we show in the next sections, in the FM phase this leads to the emergence of a gapless edge mode which carries fluctuations in ϕ_+ (physically representing rotations of the total spin in the XY plane), and is protected by an approximate conservation of the spin component S^z in the edge sector.

III. NORMAL MODES AND EFFECTIVE MODEL

The low-energy dynamics of the model discussed in the previous section is complicated by the fact that the ground-state of the system is non-uniform in the $\hat{x}$ direction due to the edge potential. In the FM phase, there are gapless low-energy excitations which are confined to the edge of the system[18], whereas all excitations in the bulk are gapped. As described above we are primarily interested in transport due to the low-energy edge excitations and how this is impacted by the bulk excitations at low but finite temperature. Accomplishing this involves the challenge of developing a theory which includes both the edge and bulk excitations, and interactions between them. A natural description of the edge modes involves tilting the spin orientations away from their semiclassical groundstate, for example using the degrees of freedom $\phi_\pm$ and their conjugates $\Pi_\pm$ in Eq. (2.11). As argued in

the last section, only gradient terms of the variable ϕ_+ can appear in the effective action, Eq. (2.12), leading to gapless modes which will dominate the low-temperature transport properties of the system[18,26].

The difficulty with using this parameterization for the entire system lies in the rather different orientations of the spins in the semiclassical ground-state configuration near the edge and deep in the bulk. The problem is apparent in Eq. (2.10). In the FM state, deep in the bulk spins are oriented along the $\hat{z}$ direction; i.e., $\psi_\nu^0 = 0$. This means that one should restrict $\Pi_\nu < 0$ for fluctuations that are physically allowable: spins can only fluctuate *downward* from this orientation. Such a constraint is very challenging to implement in a fluctuating field theory. One may prefer in this situation to retain the original spin variables, $\vec{S}_\nu$, for which $\langle S_\nu^z \rangle = 1/2$ in the ground-state, and S_ν^x, S_ν^y are conjugate variables. This is just the standard approach to spin waves[39].

Thus, there is an essential tension between the natural degrees of freedom in the bulk and at the edge. In this section we will introduce an effective model in which we write both the bulk and the edge degrees of freedom in their "natural" representations, while retaining the basic symmetries of the system, and thereby introducing couplings that will allow energy to be exchanged between the bulk and the edge.

A. Single Component Model: Ground state

We begin first with a simplified model meant to represent only the lowest energy degrees of freedom of the system, which captures both the variation of the spins at the edge and the change in the gapless mode structure as the system passes through the CAF-FM transition, but is simple enough to allow analytic progress to be made. By developing this model we will be able to gain insight into how parameters of our effective model should behave. Towards this end we introduce the energy functional

$$E[\hat{n}] = \int_{x>0} d^2r \left\{ -E_z n_z + \tilde{g} n_z^2 + \frac{\rho_0}{2} \sum_{\alpha=x,y,z} |\vec{\nabla} n_\alpha|^2 \right\}, \tag{3.1}$$

where $n(\mathbf{r})$ is a unit vector field ($\sum_\alpha n_\alpha(\mathbf{r})^2 = 1$) on the two-dimensional domain $\mathbf{r} = (x > 0, y)$. Qualitatively, one could identify this degree of freedom with the spin-1 field obtained from the symmetric combination $\mathbf{S} = \mathbf{S}_a + \mathbf{S}_b$ of the spin-1/2 fields described in Section II. Eq. (3.1) is essentially a low-energy approximation of the model given by Eqs. (2.4) and (2.7) [with $\tilde{g} \sim |g_{xy}|$], where $U(x)$ is replaced by a sharp boundary condition at $x = 0$, and $\mathbf{S}_a$, $\mathbf{S}_b$ are assumed to obey the bulk condition $\psi_a(\mathbf{r}) = \psi_b(\mathbf{r})$, $\phi_a(\mathbf{r}) = \phi_b(\mathbf{r})$ for all $\mathbf{r}$ except very close to the boundary. This model supports two phases in its bulk, a ferromagnet ($n_z = 1$) for $E_z > E_z^c \equiv 2\tilde{g}$, and a canted state ($n_z = E_z/2\tilde{g}$) for $E_z < E_z^c$. To mimic the behavior of the $\nu = 0$ system edge, we impose the boundary condition $n_z(x = 0) = -1$, which forces a domain wall (DW) at the edge into the groundstate configuration. In the FM state, the DW configuration may be found analytically with standard techniques[40]. Assuming a classical groundstate in which the unit vector rotates through the $\hat{x}$ direction in going from the bulk to edge, one writes $n_z(x) \equiv \cos\theta(x)$, $n_x(x) \equiv \sin\theta(x)$, and the configuration $\theta(x)$ that minimizes the energy functional satisfies

$$\rho_0 \frac{d^2\theta}{dx^2} = E_z \sin\theta - \tilde{g} \sin 2\theta. \tag{3.2}$$

This is equivalent to the equation of motion for a particle at "position" θ accelerating with respect to "time" x through a potential

$$V[\theta] = E_z \cos\theta - \frac{1}{2}\tilde{g} \cos 2\theta.$$

Assuming the system is in the FM state in the bulk, we must have $\theta \to 0$ as $x \to \infty$, which fixes the total energy of the fictitious particle at $E_z - \tilde{g}/2$. Using energy conservation one then finds that the particle "velocity" obeys the equation

$$\frac{d\theta}{dx} = -\frac{\left[E_z(1-\cos\theta) - \frac{1}{2}\tilde{g}(1-\cos 2\theta)\right]^{1/2}}{\sqrt{\rho_0/2}}. \tag{3.3}$$

Equation (3.3) may be recast in an integral form

$$\frac{x}{\sqrt{\rho_0/2}} = -2\int_{\pi/2}^{\theta(x)/2} \frac{d\psi}{\sin\psi \left[2E_z - 4\tilde{g}\cos^2\psi\right]^{1/2}},$$

for which the integral may be computed explicitly. Defining the length scale

$$\ell_{DW} \equiv \sqrt{\frac{\rho_0/2}{2E_z - 4\tilde{g}}} = \sqrt{\frac{\rho_0}{4(E_z - E_z^c)}}, \tag{3.4}$$

which is clearly the analog of ξ [Eq. (2.8)], this leads to the equation

$$z \equiv e^{-x/\ell_{DW}} = \left[\frac{1-\cos\theta/2}{1+\cos\theta/2}\right] \frac{E_z + 2\tilde{g}\cos\theta/2 + \sqrt{E_z - 2\tilde{g}}\sqrt{E_z - 2\tilde{g}\cos^2\theta/2}}{E_z - 2\tilde{g}\cos\theta/2 + \sqrt{E_z - 2\tilde{g}}\sqrt{E_z - 2\tilde{g}\cos^2\theta/2}}. \tag{3.5}$$

Finally, Eq. (3.5) may be inverted, which (using the boundary conditions on θ) yields the result $\cos\theta(x) = 2y^2(x)+1$, with

$$y^2(x) = \frac{1}{2\left[2\tilde{g}(1-z)^2 + r^2(1+z)^2\right]}\Bigg\{ r^2(z+1)^2 + (E_z+2\tilde{g})(z-1)^2 \qquad (3.6)$$
$$- \Big[\big(r^2(z+1)^2 + (E_z+2\tilde{g})(z-1)^2\big)^2 - 4E_z(z-1)^2\big(2\tilde{g}(1-z)^2 + r^2(1+z)^2\big)\Big]^{1/2}\Bigg\},$$

where the quantity $r \equiv \sqrt{E_z - E_z^c}$ measures how close the system is to the transition between the FM and canted phases.

The DW in this model is essentially analogous to what was found in the edge DW for the $\nu = 0$ FM state discussed in Section II. At distances from the edge larger that ℓ_{DW}, $\theta(x)$ becomes very small, and approaches zero (the bulk value for the FM state) exponentially, $\theta(x) \sim e^{-x/2\ell_{DW}}$. One can also solve for the DW shape exactly at the critical value $E_z = E_z^c$, either using the method above or by taking the $r \to 0$ limit of Eq. (3.6). The result is

$$\theta(x) \to \theta_c(x) \equiv 2\mathrm{arccot}\left[\sqrt{\frac{\tilde{g}}{\rho_0}}x\right]. \qquad (3.7)$$

B. Single Component Model: Fluctuations

We next consider the normal modes around this classical energy minimum. A simple way to proceed is to define a unit vector $\hat{n}'(x)$ such that $n'_z(x) = 1$ in the classical groundstate. This is accomplished by taking $n'_y = n_y$, and

$$\begin{pmatrix} n_x(x) \\ n_z(x) \end{pmatrix} = \begin{pmatrix} \cos\theta_{DW}(x) & \sin\theta_{DW}(x) \\ -\sin\theta_{DW}(x) & \cos\theta_{DW}(x) \end{pmatrix}\begin{pmatrix} n'_x(x) \\ n'_z(x) \end{pmatrix},$$

where $\theta_{DW}(x)$ is the DW configuration which minimizes the energy functional. Substituting this into Eq. (3.1), and writing $n'_z = \sqrt{1-n'^2_x - n'^2_y} \approx 1-(n'^2_x+n'^2_y)/2$, after some algebra one arrives at an energy functional which may be written to quadratic order in the form

$$H[\hat{n}'] \approx \sum_{\mu=x,y}\int_{x>0} d^2r\left\{n'_\mu(\mathbf{r})\left[-\frac{\rho_0}{2}\nabla^2 + U_\mu(x)\right]n'_\mu(\mathbf{r})\right\}, \qquad (3.8)$$

with "potentials"

$$U_x(x) = \frac{1}{2}E_z\cos\theta_{DW}(x) - \tilde{g}\cos 2\theta_{DW}(x), \qquad (3.9)$$
$$U_y(x) = \frac{3}{2}E_z\cos\theta_{DW}(x) - 2\tilde{g}\cos^2\theta_{DW}(x) - E_z + \tilde{g}.$$

To obtain the normal modes from this, it is convenient to impose angular momentum commutation relations on the components of the unit vector, $[n'_x(\mathbf{r}_1), n'_y(\mathbf{r}_2)] = 2i\delta(\mathbf{r}_1-\mathbf{r}_2)n'_z(\mathbf{r}_1) \approx 2i\delta(\mathbf{r}_1-\mathbf{r}_2)$. The last step, in which n'_z is replaced by its groundstate value of 1, is the spin-wave approximation[39].

The classical groundstate we have chosen in assuming the DW rotates through the $n_x - n_z$ plane is a broken symmetry state of Eq. (3.1); globally rotating the unit vector configuration around the n_z axis yields a different configuration with exactly the same energy. Because of this, the quadratic Hamiltonian [Eq. (3.8)] must host a zero mode[40]. This can be directly identified with an eigenfunction of the operator $-\frac{\rho_0}{2}\nabla^2 + U_y(x)$ with zero eigenvalue, $S_0(x)$, where $S_0(x) \equiv \sin\theta_{DW}(x)$. Note that this zero mode is confined to the region of the domain wall, and is independent of the real-space coordinate y.

Because the Hamiltonian and groundstate are uniform in the $\hat{y}$ direction, the normal modes have well-defined momentum q_y. One may exploit this by writing $n'_x(\mathbf{r}) = \int dq_y m_x(x,q_y)e^{iq_y y}/\sqrt{2\pi}$ and $n'_y(\mathbf{r}) = \int dq_y m(x,q_y)e^{-iq_y y}/\sqrt{2\pi}$. The normal mode Hamiltonian may now be written as

$$H = \int dq_y \int_0^\infty dx\Big\{m_x(x,-q_y)\left[h_x(q_y) + \frac{1}{2}\rho_0 q_y^2\right]m_x(x,q_y)$$
$$+ m_y(x,-q_y)\left[h_y(q_y) + \frac{1}{2}\rho_0 q_y^2\right]m_y(x,q_y)\Big\}, \qquad (3.10)$$

with operators $h_\mu = -\frac{1}{2}\rho_0\partial_x^2 + U_\mu(x)$. Note that we expect the effectively one-dimensional operators m to obey $m_{x,y}(x,q_y) = m_{x,y}(x,-q_y)^\dagger$. The normal modes of the system are determined by the eigenvalues and eigenfunctions of the operators $h_{x,y}$, which are difficult to determine analytically. The potentials associated with them, $U_{x,y}(x)$ [Eq. (3.9)], both reach the constant value of $E_z/2 - \tilde{g}$ at large positive x. Thus these operators will have continuous spectra of eigenvalues above this energy scale, which becomes the frequency edge for spin-waves in the bulk of the system.

C. Bulk Hamiltonian

If we wish to focus on the behavior deep in the bulk, one can simply set $U_{x,y}(x) \to E_z/2 - \tilde{g}$ and extend the domain of x to $-\infty < x < \infty$. The resulting bulk Hamil-

tonian can be written

$$H_b = \frac{1}{2}\sum_{\alpha=x,y}\int d^2r\Big[S_\alpha(\mathbf{r})\left(E_z - 2\tilde{g} - \rho_0\nabla^2\right)S_\alpha(\mathbf{r})\Big], \tag{3.11}$$

where we have made the identification $m_\alpha(\mathbf{r}) \equiv S_\alpha(\mathbf{r})$, the components of the unit vector in real space. H_b supports a gapped spin-wave mode of frequency $\omega(q) = E_z - 2\tilde{g} + \rho_0 q^2$ which becomes gapless at the phase transition, i.e. when E_z acquires the critical value $E_z^c = 2\tilde{g}$; this behavior is highly analogous to what is found for the low energy modes in the full system near the transition in time-dependent Hartree-Fock calculations[35]. Alternatively, one may rewrite Eq. (3.11) in terms of bosonic raising and lowering operators, $a(\mathbf{r}) = (S_x(\mathbf{r}) + iS_y(\mathbf{r}))/\sqrt{2}$, $a^\dagger(\mathbf{r}) = (S_x(\mathbf{r}) - iS_y(\mathbf{r}))/\sqrt{2}$, which upon taking the ferromagnetic groundstate average for the S_z component of the spin[39] yields the needed commutation relations $[a(\mathbf{r}), a^\dagger(\mathbf{r}')] = \delta(\mathbf{r}-\mathbf{r}')$, so that

$$H_b = \int d^2r\left[-\frac{1}{2}\rho\left(a^\dagger(\mathbf{r})\nabla^2 a(\mathbf{r}) + a(\mathbf{r})\nabla^2 a^\dagger(\mathbf{r})\right) + \Delta a^\dagger(\mathbf{r})a(\mathbf{r})\right]. \tag{3.12}$$

In writing Eq. (3.12) we have dropped the subscript 0 in ρ_0, and

$$\Delta = E_z - 2\tilde{g} = E_z - E_z^c\,. \tag{3.13}$$

Note that we expect H_b more generally to be the long-wavelength form of the Hamiltonian governing the low energy modes deep in the bulk of the FM state of the $\nu = 0$ quantum Hall state, with $\Delta \to 0$ as the transition to the CAF state is approached.

D. Edge Hamiltonian

We next turn to a discussion of the lowest energy mode of the FM phase, which as discussed above is a gapless edge state mode. Near the edge, U_y of Eq. (3.9) has a well potential which monotonically increases with increasing x towards its asymptotic value. It is also interesting to note that $U_x = U_y + \Delta U$, with $\Delta U = E_z[1 - \cos\theta_{DW}(x)] \geq 0$, so that $U_x(x) \geq U_y(x)$ for any x. Presuming our domain wall structure is stable, there cannot be any negative energy states associated with either h_x or h_y in Eq. (3.10). We have seen that for $q_y = 0$, h_y supports a zero energy state; this is unlikely to be the case for h_x because the effective potential associated with it is larger than that of h_y. It is possible that there are bound states in the spectral interval $[0, E_z/2 - \tilde{g}]$, but as the critical value of E_z is approached this becomes a very small interval and so is unlikely to host any bound states. Thus we assume that there is only one bound state in the spectra of h_x and h_y for $q_y = 0$, associated with h_y, at zero eigenvalue. With increasing q_y there will be a single linearly dispersing mode, which we associate with the gapless edge excitation of the system. Then the lowest energy modes of the system in the FM phase are the single gapless edge mode and the bulk spin wave modes discussed in subsection C. We note that the absence of other low-energy modes is in apparent agreement with time-dependent Hartree-Fock results for the full $\nu = 0$ spectrum[35].

In order to write down an effective Hamiltonian for the edge mode it is useful to consider the equations of motion for $m_y(x)$ and $m_y(x)$. Using $\partial_t\mathcal{O} = i[H, \mathcal{O}]$, we find

$$\begin{aligned}\partial_t m_x &= 4(h_y + \frac{1}{2}\rho_0 q_y^2)m_y \\ \partial_t m_y &= -4(h_x + \frac{1}{2}\rho_0 q_y^2)m_x.\end{aligned}$$

The two equations can be combined to give, after Fourier transforming with respect to time,

$$\omega^2 m_y = 16(h_x + \frac{1}{2}\rho_0 q_y^2)(h_y + \frac{1}{2}\rho_0 q_y^2)m_y. \tag{3.14}$$

For $q_y = 0$ this equation is solved by $m_y = S_0(x)$ and $\omega = 0$, and we are interested in the solution that smoothly joins to this in the limit $q_y \to 0$. To quadratic order in q_y, this may be written in real time as $m_y(q_y, t) = [S_0(x) + \delta S(x, q_y)]\phi(q_y, t)$, with δS of order q_y^2. Using the fact that $h_y S_0(x) = 0$, the equation of motion to order q_y^2 becomes

$$-\partial_t^2 S_0(x)\phi(q_y,t) = 16[h_x h_y \delta S(x,q_y) + \frac{1}{2}\rho_0 q_y^2 h_x S_0(x)]\phi(q_y,t). \tag{3.15}$$

Recalling our assumption that h_x does not support a zero mode, it will have a well-defined inverse operator h_x^{-1} which we can apply to Eq. (3.15). Finally, multiplying the whole equation by $S_0(x)$ on the left, integrating with respect to x, and using the fact that $\langle S_0|h_y|\delta S\rangle \equiv \int_0^\infty dx S_0(x)h_y\delta S(x) = 0$ for any δS, we obtain the equation of motion

$$\left[-8\rho_0 q_y^2 - \langle S_0|h_x^{-1}|S_0\rangle\partial_t^2\right]\phi(q_y,t) = 0. \tag{3.16}$$

Thus we find a linearly dispersing normal mode $\omega(q_y) = u_0 q_y$, with velocity $u_0 = \sqrt{8\rho_0/\langle S_0|h_x^{-1}|S_0\rangle}$.

The gapless edge mode obtained above is the only mode in the FM phase that approaches zero energy. The variable ϕ represents an amplitude to rotate the spins of the DW into the $\hat{y}$ axis from the $\hat{x}$ axis through which we assumed the spins spatially rotate in the classical DW groundstate. Qualitatively, one may associate it with an azimuthal angle of the spins at the center of the DW, and it plays a role highly analogous to the ϕ_+ degree of freedom in Section II. Quantizing this degree of freedom leads to a standard Luttinger liquid Hamiltonian, which, after Fourier transforming into real space, may be written in the form

$$H_e = \frac{u_{_{NM}}}{2\pi} \int dy \left\{ K_{_{NM}} \left(\pi \Pi(y)\right)^2 + \frac{1}{K_{_{NM}}} \left(\partial_y \phi(y)\right)^2 \right\}, \tag{3.17}$$

with $[\Pi(y), \phi(y')] = -i\delta(y - y')$, and $u_{_{NM}} = u_0$. Note that because Π and ϕ are conjugate, the former can be identified with deviations of spins near the center of the DW into the S_z direction, as expected from the general considerations of Section II. Because the energy cost for spatial gradients in ϕ descends directly from the two-dimensional spin stiffness ρ_0, we expect $u_{_{NM}}/\pi K_{_{NM}} \sim \rho_0$, which remains finite and non-vanishing even as the transition point is approached (i.e., when the gap Eq. (3.13) obeys $\Delta \to 0$). This implies that the Luttinger parameter behaves as

$$K_{_{NM}}^{-1} \sim \frac{\pi}{2} \left(\rho_0 \langle S_0 | h_x^{-1} | S_0 \rangle\right)^{1/2}. \tag{3.18}$$

Two comments are in order. First, as explained in Appendix A, $\langle S_0 | h_x^{-1} | S_0 \rangle \sim \Delta^{-1/2}$, which is divergent as $\Delta \to 0$, so that the Luttinger parameter K vanishes in this limit. This means that the edge mode becomes extremely sensitive to perturbations at the edge (in the renormalization group sense), so that the edge Luttinger liquid cannot remain stable as the bulk transition from a FM to a CAF phase is approached. Secondly, the behavior of the coefficients of the edge theory as the system approaches the transition point are chosen to match what is found in the normal mode theory. Going beyond this to include coupling terms between the bulk and edge modes will be most naturally accomplished by writing them in a way that includes quadratic contributions, so that this edge-bulk coupling leads to significant contributions to the edge theory. Rather than deviate from our development of our effective model, we defer a fuller discussion of this to Appendix A. At this point, we introduce our model of the edge-bulk coupling.

E. Bulk-Edge Coupling

As described in Sec. I, the gapless edge mode of this system is in fact a helical, charge-carrying mode. Spin waves described by the effective one-dimensional theory above should be understood as carrying current in the positive or negative direction, with amplitude proportional to the deviation of the expectation value of S_z in the excited state from its groundstate value. As in other topological systems[17], dissipation at zero temperature in this edge system is then suppressed because backscattering requires spin-flip, which cannot be accomplished by static disorder[18,19]. At finite temperature, however, spin waves will always be present in the bulk, so that the edge system can exchange angular momentum with it.

We thus introduce a phenomenological coupling which captures this process and respects conservation of angular momentum, in the form

$$H_{int} = g \int dy \left\{ a^\dagger(0,y) e^{i\phi(y)} + a(0,y) e^{-i\phi(y)} \right\}. \tag{3.19}$$

Recalling that the bulk bosonic operators are actually spin raising and lowering operators ($a = (S_x + iS_y)/\sqrt{2}$, $a^\dagger = (S_x - iS_y)/\sqrt{2}$), one sees that the two terms in H_{int} respectively flip a spin down and up in the degrees of freedom associated with H_b, at $x = 0$, which is treated as the location of the DW. Compensating these spin flip operators are the operators $e^{\pm i\phi(y)}$, which represent the opposing spin flips in the edge system H_e. This is easily understood when one recalls that the $\Pi(y)$ operator represents the deviation of S_z from its groundstate configuration due to excitation of edge modes, and one may verify that $e^{\pm i\phi(y)}$ are raising/lowering operators with respect to the Π operator[42]. The two terms in H_{int} thus each conserve S_z in the system as a whole ($H_b + H_e$).

Finally, we note that our full effective model, $H_b + H_e + H_{int}$, can be expanded around a classical groundstate configuration to produce the normal modes of the system. To be consistent, modes deep in the bulk and at the edge should behave as $\Delta \to 0^+$ in the same way as what we found for the model introduced at the beginning of this section. This analysis is discussed in more detail in App. A. It leads to the conclusion that the effective "bare" Luttinger parameter K and spin wave velocity u in H_e scale with Δ in the same way as those in the normal mode theory, and the phenomenological constant g vanishes with Δ. Specifically one finds

$$\begin{aligned} u &\sim \Delta^{1/4}, \\ K &\sim \Delta^{1/4}, \\ g &\sim \Delta^{3/4}. \end{aligned} \tag{3.20}$$

With this scaling one finds among the normal modes for the fully coupled bulk-edge system a gapless spin-wave mode, at the edge, with velocity scaling as $\Delta^{1/4}$, as found for the simple model developed at the beginning of this section.

With this phenomenological model, we are now in a position to understand how the coupling between the edge and bulk can impact transport in the ferromagnetic state.

IV. CONDUCTANCE

We now turn to the calculation of electric conductance, and investigate its dependence on temperature (T) and the Zeeman energy E_z. The results can be compared to the two-terminal conductance data of Ref. 32, and to potentially more systematic future studies at low T. We note that in both the CAF and FM phases, the lowest energy charged excitations are edge modes, and these are expected to dominate the d.c. electric transport. However, in the CAF the edge modes are still gapped, and the conductance at finite T is therefore expected to exhibit an activated behavior of the form

$$G(E_z < E_z^c) \sim e^{-\Delta_c/T}, \tag{4.1}$$

where Δ_c has been shown[34] to vanish when approaching the transition as $\Delta_c \sim (E_z^c - E_z)\log(E_z^c - E_z)$. We therefore focus on the behavior in the FM phase, where the edge mode is gapless and naively one expects perfect conduction. Interestingly, as we show below, in this phase the *resistivity* at finite T exhibits a similar activated form, reflecting a "duality relation" between the two phases.

Our starting point is the effective Hamiltonian derived in the previous section:

$$\begin{aligned} H_{eff} &= H_e + H_b + H_{int} \qquad (4.2)\\ H_e &= \frac{u}{2\pi}\int \mathrm{d}y \left\{ K\left(\pi\Pi\right)^2 + \frac{1}{K}\left(\partial_y\phi\right)^2 \right\},\\ H_b &= \int \mathrm{d}^2 r \left\{ -\frac{1}{2}\rho\left(a^\dagger\nabla^2 a + a\nabla^2 a^\dagger\right) + \Delta a^\dagger a \right\},\\ H_{int} &= g\int \mathrm{d}y \left\{ a^\dagger\left(0,y\right)e^{i\phi(y)} + a\left(0,y\right)e^{-i\phi(y)} \right\}, \end{aligned}$$

which describes a helical Luttinger liquid coupled to a bath of 2D massive bosons along the line $x = 0$. For simplicity, we assume here the 2D bulk to be an infinite plane rather than the semi-infinite plane $x > 0$ considered in App. A: a straightforward calculation shows that the effect of bulk-edge coupling in the two cases is the same for an appropriate definition of the coupling constant g. The local bosonic fields $a(\mathbf{r})$, $a^\dagger(\mathbf{r})$ correspond, in the spin-wave approximation, to the bulk spin operators $S^-(\mathbf{r})$, $S^+(\mathbf{r})$, respectively; the canonically conjugate operators $\phi(y)$, $\Pi(y)$ encode, respectively, the planar angle and spin density $S_e^z(y)$ on the edge. We recall that the last term, representing the most relevant coupling between edge and bulk modes, can be traced back to a spin-flip term of the form $(S_b^+ S_e^- + h.c.)$.

To the Hamiltonian describing the clean system Eq. (4.2), we next add a term which accounts for the coupling to a random potential associated with static impurities,

$$H_{dis} = -\int \mathrm{d}y \mu\left(y\right)\rho_e(y) = \frac{1}{\pi}\int \mathrm{d}y \mu\left(y\right)\partial_y\phi, \tag{4.3}$$

where in the last step we have used the expression for the edge density operator in terms of the bosonic field ϕ. Note that the helicity of the edge mode forbids standard backscattering terms [e.g. $\cos(2\phi)$] which would normally dominate the relaxation of charge current on the edge j_e by direct coupling of left and right moving components. In the absence of coupling to the bulk via the term H_{int} in Eq. (4.2), the edge mode thus obeys conservation of the total spin operator $\mathcal{S}_e^z = \int \mathrm{d}y\, S_e^z(y)$, which is equivalent to the d.c. component of the charge current,

$$J_e = \int \mathrm{d}y\, j_e(y) = Ku\int \mathrm{d}y\, \Pi(y)\,. \tag{4.4}$$

The forward scattering term Eq. (4.3) can be absorbed into a redefinition of ϕ by the transformation[42,43] $\phi\left(y\right) \to \phi\left(y\right) + (K/u)\int_0^y \mathrm{d}y' \mu\left(y'\right)$ leading to a random phase shift of the operators appearing in H_{int}:

$$\begin{aligned} e^{i\phi(y)} &\to e^{i\phi(y)}\zeta\left(y\right)\ ,\\ \zeta\left(y\right) &\equiv e^{i(K/u)\int_0^y \mathrm{d}y' \mu\left(y'\right)}\ . \end{aligned} \tag{4.5}$$

For a generic disorder potential, the random variable $\zeta\left(y\right)$ can be assumed to satisfy

$$\left\langle \zeta\left(y\right)\right\rangle_{dis} = 0, \quad \left\langle \zeta\left(y\right)\zeta^*\left(y'\right)\right\rangle_{dis} = D\delta\left(y - y'\right), \tag{4.6}$$

where $\langle \ldots \rangle_{dis}$ denotes an average over disorder.

The two-terminal conductance G is next evaluated under the assumption that due to the almost conservation of $\mathcal{S}_e^z$ (and hence J_e) on each of the two edges, the intrinsic electric resistivity is small; i.e., in units of e^2/h,

$$G = \frac{2}{R_0 + \delta R} \tag{4.7}$$

where $R_0 \approx 1$ is the contact resistance arising from coupling of the leads to a single 1D channel, and $\delta R \ll 1$. Deviations of R_0 from the ideal value $R_0 = 1$ due to extrinsic processes (e.g., spin-relaxation in the contacts) reduces G from the perfect $G = 2$ value but may be assumed to have a negligible T-dependence. The intrinsic contribution $\delta R = L/\sigma$ (where L is the length of the sample in the edge direction and σ is the d.c. conductivity) is treated perturbatively in the rate of scattering.

To this end, we employ a hydrodynamic approximation[44] of the Kubo formula for σ,

$$\sigma = \lim_{\omega\to 0}\frac{1}{L\omega}\int_0^\infty \mathrm{d}t\, e^{i\omega t}\langle[J_e(t), J_e(0)]\rangle \tag{4.8}$$

(the ee component of the conductivity matrix $\hat{\sigma}$ in a basis of current operators $\{J_p\}$), whereby it can be recast in terms of the inverse of a memory matrix $\hat{M}$, encoding relaxation rates:

$$\hat{\sigma} = \hat{\chi}[\hat{M}]^{-1}\hat{\chi}\,. \tag{4.9}$$

Here $\hat{\chi}$ is the matrix of static susceptibilities

$$\chi_{pq} = \frac{1}{L}\int_0^\beta \mathrm{d}\tau\, \langle J_p(\tau)J_q(0)\rangle \equiv (J_p|J_q) \tag{4.10}$$

(describing an "overlap" of the operators J_p, J_q), and $\hat{M}$ is determined by correlation functions of the force operators

$$F_p = \dot{J}_p = i[H, J_p] \; ; \tag{4.11}$$

generally, the explicit form of $\hat{M}$ is quite complicated[44], however in the case where $(F_p|J_p) = 0$ it greatly simplifies and

$$\begin{aligned} M_{pq} &= \lim_{\omega\to 0} \frac{C_{pq}(\omega) - C_{pq}(\omega = 0)}{i\omega} \; , \\ C_{pq}(\omega) &= \frac{-i}{L}\int_0^\infty \mathrm{d}t e^{i\omega t}\langle [F_p(t), F_q(0)]\rangle \; . \end{aligned} \tag{4.12}$$

In Eqs. (4.8) through (4.12), $\langle ...\rangle$ denotes thermal expectation value at temperature T. It is apparent from Eq. (4.9) that the matrix elements of $\hat{\sigma}$ are dominated by slow modes, for which F_p and hence the the matrix element M_{pp} is small. In particular, the presence of a conserved operator J_c which commutes with the Hamiltonian (i.e. $F_c = 0$) leads to the divergence of any physical conductivity σ_{pp} (and hence vanishing of the resistivity) provided the cross susceptibility $\chi_{pc} \neq 0$; in such a case, the current J_p is protected by the conservation law and can not decay[45]. When the conservation law is only approximate, one obtains a finite relaxation rate dominated by the small memory matrix element M_{cc}.

In our case, the approximate conservation law protecting the charge current on each edge is $\mathcal{S}^z_e$, which is identical to J_e up to a constant prefactor [Eq. (4.4)][46]. This justifies a diagonal version of Eq. (4.9) and one obtains

$$\delta R = \frac{L}{\sigma} = \frac{LM_{ee}}{\chi^2_{ee}}, \tag{4.13}$$

where, for a Luttinger liquid, χ_{ee} is easily computed[42] to yield a constant $\chi_{ee} = 2uK/\pi$. Employing Eq. (4.12) for $p = q = e$ (and a standard identity for the retarded correlation function) we get

$$\delta R = -\frac{1}{2(uK/\pi)^2}\int_0^\infty \mathrm{d}t\, t\Im m\{\langle F_e(t)F_e(0)\rangle\} \tag{4.14}$$

where, substituting Eq. (4.2) for the effective Hamiltonian,

$$F_e = i[H_{eff}, J_e] = i[H_{int}, J_e] \; ; \tag{4.15}$$

in the last step we have used $[H_e, J_e] = 0$. The intrinsic resistivity is therefore dominated by processes whereby the edge spin is relaxed into the 2D bulk. We finally introduce the disorder potential by performing the phase shift Eq. (4.5), so that H_{int} acquires the form

$$H_{int} = g\int \mathrm{d}y \left\{\zeta(y)a^\dagger(0,y)\, e^{i\phi(y)} + \zeta^*(y)a(0,y)\, e^{-i\phi(y)}\right\}. \tag{4.16}$$

Evaluating δR from Eq. (4.14) to leading order in H_{int} [Eq. (4.16)], we modify the definition of angular brackets $\langle ...\rangle$ to include the disorder averaging $\langle ...\rangle_{dis}$.

We next employ Eqs. (4.4), (4.15) and (4.16) to get the correlation function

$$\begin{aligned} \langle F_e(t)F_e(0)\rangle &= (guK)^2\int \mathrm{d}y\int \mathrm{d}y'\,\langle\zeta(y)\zeta^*(y')\rangle_{dis}\left\langle e^{i\phi(y,t)}e^{-i\phi(y',0)}\left\{a^\dagger(0,y,t)\,a(0,y',0) + a(0,y,t)\,a^\dagger(0,y',0)\right\}\right\rangle \\ &\approx (guK)^2 D\int \mathrm{d}y\langle e^{i\phi(y,t)}e^{-i\phi(y,0)}\rangle_e\left\{\langle a^\dagger(0,y,t)\,a(0,y,0)\rangle_b + \langle a(0,y,t)\,a^\dagger(0,y,0)\rangle_b\right\}, \end{aligned} \tag{4.17}$$

where in the last step we have used Eq. (4.6), and maintain the leading order in g for which the thermal expectation value is evaluated with respect to $H_0 = H_e + H_b$ (where the bulk and edge sectors are decoupled). Both sectors are described by free bosonic theories [see Eq. (4.2)]. The edge part of the correlation function is given by the standard result for a Luttinger liquid[42],

$$\langle e^{i\phi(y,t)}e^{-i\phi(y,0)}\rangle_e = \lim_{\epsilon\to 0}\frac{\left(\frac{\pi\alpha}{\beta u}\right)^{K/2}(-1)^{-K/4}}{\left[\sinh\left(\frac{(t-i\epsilon)\pi}{\beta}\right)\right]^{K/2}}, \tag{4.18}$$

where α is a short-distance cutoff. For the bulk, we use the bosonic correlation functions in momentum space

$$\begin{aligned} \langle a^\dagger_{\mathbf{k}}(t)a_{\mathbf{k}'}(0)\rangle_b &= e^{i\omega_{\mathbf{k}}t}n_{_B}(\mathbf{k})\delta_{\mathbf{k},\mathbf{k}'} \; , \\ \omega_{\mathbf{k}} &= \Delta + \rho|\mathbf{k}|^2, \end{aligned} \tag{4.19}$$

where $n_{_B}(\mathbf{k}) = 1/(e^{\beta\omega_{\mathbf{k}}} - 1)$ is the Bose function, and similarly

$$\langle a_{\mathbf{k}}(t)a^\dagger_{\mathbf{k}'}(0)\rangle_b = e^{-i\omega_{\mathbf{k}}t}[1 + n_{_B}(\mathbf{k})]\delta_{\mathbf{k},\mathbf{k}'} \; . \tag{4.20}$$

The local correlation functions thus become

$$\langle a^\dagger(0,y,t)\, a(0,y,0)\rangle_b = \int \mathrm{d}^2k\, e^{i\omega_{\mathbf{k}}t} n_{_B}(\mathbf{k}), \qquad (4.21)$$
$$\langle a(0,y,t)\, a^\dagger(0,y,0)\rangle_b = \int \mathrm{d}^2k\, e^{-i\omega_{\mathbf{k}}t}[1+n_{_B}(\mathbf{k})]\ .$$

Inserting Eqs. (4.21) and (4.18) into (4.17) we obtain for δR [Eq. (4.14)]:

$$\delta R \approx -\mathcal{D}\int_0^\infty \mathrm{d}t\, t\Im m\{\mathcal{C}(t)\}\ , \quad \text{where} \qquad (4.22)$$
$$\mathcal{D} \equiv \frac{\pi^2 g^2 DL}{2}\left(\frac{\pi\alpha}{\beta u}\right)^{K/2}\ , \quad \mathcal{C}(t) \equiv \lim_{\epsilon\to 0}\frac{(-1)^{-K/4}}{\left[\sinh\left(\frac{(t-i\epsilon)\pi}{\beta}\right)\right]^{K/2}}\int\frac{\mathrm{d}^2k}{(2\pi)^2}\left\{e^{i\omega_{\mathbf{k}}t}n_{_B}(\mathbf{k}) + e^{-i\omega_{\mathbf{k}}t}[1+n_{_B}(\mathbf{k})]\right\}\ .$$

Note that $D \propto n_{imp}$ where n_{imp} is the density of impurities per unit length; hence, the factor DL encodes the number of impurities N_{imp}. Performing the integrals in Eq. (4.22) we obtain (see Appendix B for details)

$$\delta R = \frac{2^{\frac{K}{2}}\mathcal{D}\beta}{8\pi^2\rho}\frac{\Gamma\left(1-\frac{K}{2}\right)\sin\left(\frac{\pi K}{2}\right)}{2\pi} f(\beta\Delta)\ ,$$
$$f(z) \equiv \int_z^\infty \mathrm{d}x \left|\Gamma\left(\frac{K}{4}+i\frac{x}{2\pi}\right)\right|^2 \frac{e^{-\frac{1}{2}x}}{1-e^{-x}}\ . \qquad (4.23)$$

Recalling the T-dependence of $\mathcal{D}$ [Eq. (4.22)], this yields δR as a function of T for arbitrary values of the other parameters:

$$\delta R(T) \propto T^{\frac{K}{2}-1} f(\Delta/T)\ . \qquad (4.24)$$

In Fig. 1 we present G vs. T obtained directly from Eqs. (4.7) and (4.23), for several values of Δ corresponding to a range of E_z in the regime $E_z > E_z^c$.

We now consider the low T limit where $T \ll \Delta$, and use the asymptotic form of $f(z)$ at large argument to obtain the leading T-dependent contribution to the resistance (see App. B):

$$\delta R(T) \approx R_{int} e^{-\Delta/T}\ , \qquad (4.25)$$
$$R_{int} \equiv \frac{\pi\Gamma\left(1-\frac{K}{2}\right)\sin\left(\frac{\pi K}{2}\right)DL}{8\rho}\frac{g^2}{\Delta}\left(\frac{\alpha\Delta}{u}\right)^{K/2}\ ,$$

where we note that the prefactor of the exponential R_{int} is T-independent. This simple activation of the resistance is remarkably reminiscent of the *conductance* in the CAF phase [Eq. (4.1)], where here the activation energy $\Delta \propto (E_z - E_z^c)$ [see Eq. (3.13)] corresponds to the gap for spin-wave excitations in the bulk. Interestingly, the role it plays here is equivalent to a superconducting gap. The final expression for the low-T two-terminal conductance in the FM phase is obtained by substituting Eq. (4.25) into (4.7), yielding

$$G(E_z > E_z^c) \approx \frac{2}{R_0 + R_{int}(\Delta)e^{-\Delta/T}}, \qquad (4.26)$$

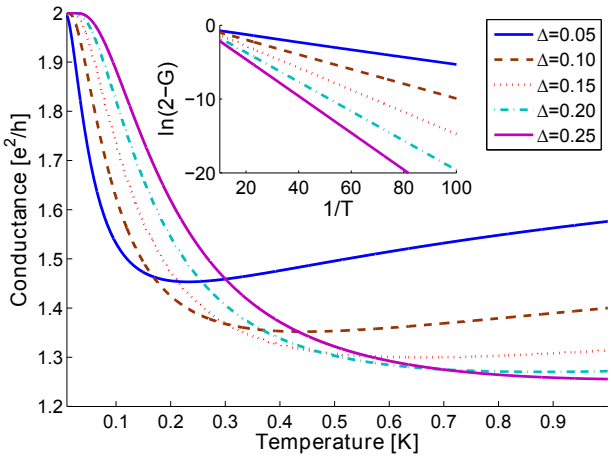

FIG. 1: (Color online.) Conductance in units of e^2/h as a function of T, for different values of Δ in units of Kelvin. Assuming that $E_z^c \sim 1$K, we take $R_0 = 1$, $K = \Delta^{1/4}$, $u = u_0\Delta^{1/4}$ and $g = g_0\Delta^{3/4}$ where u_0, g_0 are such that the overall Δ-independent prefactor of δR [Eq. (4.23)] is 0.1. Inset: zoom on the low-T regime 0.01K$\leq T \leq$ 0.1K.

where the E_z-dependence is dominated by the behavior of Δ .

V. SUMMARY

In this work we have developed an effective model for the ferromagnetic $\nu = 0$ quantized Hall state of graphene, and used it to analyze the transport behavior of the system at finite temperature. The model includes a bulk system supporting a gapped spin wave mode, an edge system supporting a charged gapless helical mode, and a coupling term allowing an exchange of spin between the two systems. In principle the parameters of the effective theory which couples the edge and bulk are free. However, we use several ways to constrain them, especially

in the ferromagnetic phase near the transition. We develop a simple nonlinear theory of the edge in the FM phase and match the E_Z-dependence of the spin-wave velocity of this model with the linear approximation to our effective theory. We further make the physical demand that the spin stiffness should neither diverge nor vanish at the transition. This completely constrains the E_Z-dependence of all the free parameters of the effective theory. An analysis in terms of the memory matrix approach allows us to determine the temperature-dependence of edge transport in this system. In the presence of disorder, charged modes of the system can be backscattered, with the necessary angular momentum for such processes within a helical channel supplied by the bulk spin excitations. This leads to concrete predictions for a two-terminal resistance measurement of the system.

Our analysis leaves open a number of interesting further questions. What is the effect of disorder on the bulk of the system? In particular, is there a range of parameters for which gapless or nearly gapless spin excitations persist in the bulk, leading to dissipative behavior over a broad range of temperatures and/or Zeeman energies? Our model can be easily generalized to capture the canted antiferromagnetic phase, which is presumably seen as an insulating state in experiments with relatively weaker Zeeman coupling. Our approach in principle allows one to compute the temperature dependence of transport in this phase as well. More challenging, and potentially very interesting, would be the transport behavior of the system through the transition itself. Connected to this, it would be generally interesting to understand the bulk properties of the system in the critical regime. How the system behaves upon doping is yet another interesting direction, an understanding of which would allow further connection of our model with existing experimental data. These and related questions will be addressed in future work.

Acknowledgements – Useful discussions with E. Andrei, N. Andrei, T. Grover, P. Jarillo-Herrero, R. Shankar and A. Young are gratefully acknowledged. The authors thank the Aspen Center for Physics (NSF Grant No. 1066293) for its hospitality. This work was supported by the US-Israel Binational Science Foundation (BSF) grant 2012120 (ES, GM, HAF), the Israel Science Foundation (ISF) grant 231/14 (ES), by NSF Grant Nos. DMR 1306897 (GM), DMR-1506263 (HAF), and DMR-1506460 (HAF).

Appendix A: Renormalization of edge parameters near criticality

In this Appendix we discuss some technical details that determine how various parameters of our effective model scale with Δ. In particular we demonstrate that the matrix element $\langle S_0|h_x^{-1}|S_0\rangle$ scales as $\Delta^{-1/2}$, as was stated in Section III D. We then discuss how this leads to the scaling of the parameters u, K, and g in our effective Hamiltonian.

1. Small Δ behavior of $\langle S_0|h_x^{-1}|S_0\rangle$

We recall the operator $h_x \equiv -\frac{1}{2}\rho_0\partial_x^2 + U_x(x)$, with

$$U_x(x) = \frac{1}{2}E_z\cos\theta_{DW}(x) - \tilde{g}\cos 2\theta_{DW}(x),$$

which has the asymptotic property $U_x(x\to\infty) = E_z/2 - \tilde{g} \equiv \Delta/2$. As discussed in Section III D, we assume for small Δ that h_x has no bound states, in particular no zero energy states, so that the operator h_x^{-1} is well-defined. The spectrum of h_x then supports only scattering states, which can be specified by eigenvalues of the form $\frac{1}{2}\rho_0 k_x^2 + \Delta/2$, with k_x formally a continuous set of parameters labeling the spectrum. Labeling the corresponding eigenvectors as $|k_x\rangle$, we then have

$$\langle S_0|h_x^{-1}|S_0\rangle = L_x\int_0^\infty \frac{dk_x}{2\pi}\frac{|\langle S_0|k_x\rangle|^2}{\frac{1}{2}\rho_0 k_x^2 + \Delta/2}, \qquad \text{(A1)}$$

where L_x is a size scale which is taken to infinity in the thermodynamic limit. We next argue that the matrix element $\langle S_0|k_x\rangle$ is finite for any Δ, including at the critical value $\Delta = 0$. Since the wavefunctions $\psi_{k_x}(x) = \langle x|k_x\rangle$ are increasingly unaffected by U_x as $\Delta\to 0$, it is sufficient to show that the matrix element is finite in this limit. Because the wavefunctions in Eq. (A1) are normalized, it is clear that the integrand is finite for large k_x and that the integral converges at its upper limit. To see that there is no divergence at the lower limit, we identify a length scale η above which the domain wall configuration $\theta_{DW}(x)$ is not appreciably different than zero, so that for $x > \eta$ we can use an asymptotic scattering form for $\psi_{k_x}(x)$, as well as $S_0(x) \approx 2\sqrt{2\rho_0/\tilde{g}}/x \equiv \xi/x$ [see Eq. (3.7)]. Writing $x = u/k_x$, the matrix element takes the form

$$\langle S_0|k_x\rangle \approx \frac{const.}{\sqrt{L_x}} + \frac{\xi}{\sqrt{L_x}}\int_{k_x\eta}^\infty du\frac{e^{-iu} - e^{iu}e^{-2i\delta(k_x)}}{u},$$

where $\delta(k_x)$ is the phase shift, which for small k_x has the form $\delta(k_x) \approx -k_x a$, with a the scattering length. It is clear from these forms that $\langle S_0|k_x\rangle$ is finite in the limit $k_x\to 0$, and we write this limit as $C/\sqrt{L_x}$. Finally, noting that, for small Δ, Eq. (A1) is dominated by the lower limit on k_x, we find

$$\langle S_0|h_x^{-1}|S_0\rangle \sim \int_0^\infty dk_x\frac{C^2}{\rho_0 k_x^2 + \Delta/2} \sim 1/\sqrt{\Delta},$$

which leads to the $u_{NM}\sim\Delta^{1/4}$ behavior discussed in Section III D.

2. Scaling of u, K, and g with Δ

We next discuss how the parameters specifying the one-dimensional part of our effective Hamiltonian, u and K, behave as the transition to the canted antiferromagnet (CAF) is approached from the ferromagnetic (FM) side. Our approach is specifically to expand the Hamiltonian for small fluctuations around a classical groundstate, and to specify the behavior of u and K to match what was found in Section III. We begin by rewriting the effective Hamiltonian in the form

$$\begin{aligned} H_{eff} &= H_e + H_b + H_{int}, \qquad \text{(A2)} \\ H_e &= \frac{u}{2\pi}\int \mathrm{d}y \left\{ K\left(\pi\Pi\right)^2 + \frac{1}{K}\left(\partial_y\phi\right)^2 \right\}, \\ H_b &= \int \mathrm{d}^2 r \left\{ \frac{1}{2}\rho\left(\vec{\nabla} a^\dagger \vec{\nabla} a + \vec{\nabla} a \vec{\nabla} a^\dagger \right) + \Delta a^\dagger a \right\}, \\ H_{int} &= g\int \mathrm{d}y \left\{ a^\dagger\left(0,y\right) e^{i\phi(y)} + a\left(0,y\right) e^{-i\phi(y)} \right\}. \end{aligned}$$

The Hamiltonian has a global symmetry of the form $\phi(y) \to \phi(y) + \varphi_0$, $a \to a e^{i\varphi_0}$, $a^\dagger \to a^\dagger e^{-i\varphi_0}$. This implies that classical groundstates form a degenerate continuous manifold, and for convenience we consider fluctuations around $\phi(y) = 0$. For small but non-vanishing values of this field, to quadratic order one finds

$$H_{int} \approx g\int dy \left\{ [a + a^\dagger][1 - \frac{1}{2}\phi(y)^2] + i\phi(y)[a^\dagger - a] \right\}. \qquad \text{(A3)}$$

Rewriting $a(\mathbf{r}) \equiv [P(\mathbf{r}) + iQ(\mathbf{r})]/\sqrt{2}$, $a(\mathbf{r})^\dagger \equiv [P(\mathbf{r}) - iQ(\mathbf{r})]/\sqrt{2}$ (i.e., P and Q denote the spin operators S_x and S_y, respectively) with $[P(\mathbf{r}_1), Q(\mathbf{r}_2)] = i\delta(\mathbf{r}_1 - \mathbf{r}_2)$, yields

$$H_{int} \approx \sqrt{2}g\int dy \left\{ P(0,y)[1 - \frac{1}{2}\phi(y)^2] + \phi(y)Q(0,y) \right\}. \qquad \text{(A4)}$$

If P is treated classically, it is clear that the Hamiltonian will be minimized by $P(\mathbf{r}) \neq 0$. Collecting terms involving P for $\phi = 0$, the function doing so will minimize

$$H_P = \int_{x\geq 0^-} d^r \left\{ \frac{1}{2}\rho|\vec{\nabla}P|^2 + \frac{1}{2}\Delta P^2 + \sqrt{2}gP(\mathbf{r})\delta(\mathbf{x}) \right\}.$$

Minimizing this subject to the boundary condition $\partial_x P(x = 0^-, y)) = 0$, which is appropriate to an open boundary, one finds $P = P_0$ with

$$\begin{aligned} P_0(x) &= \frac{-\sqrt{2}g}{\sqrt{\rho\Delta}} \qquad 0^- < x \leq 0, \\ &= \frac{-\sqrt{2}g}{\sqrt{\rho\Delta}} e^{-\left(\frac{\Delta}{\rho}\right)^{1/2} x} \quad x > 0. \end{aligned}$$

Writing $P = P_0 + p$, the effective Hamiltonian at the quadratic level now has the form

$$\begin{aligned} H_{eff} &\approx \int_{x>0^-} d^2 r \left\{ \frac{1}{2}\rho\left(|\vec{\nabla}p|^2 + |\vec{\nabla}Q|^2 \right) + \frac{1}{2}\Delta\left(p^2 + Q^2\right) \right\} \\ &+ g\int dy \left\{ \frac{g}{\sqrt{\rho\Delta}}\phi(y)^2 + \sqrt{2}\phi(y)Q(0,y) \right\} \\ &+ \frac{u}{2\pi}\int dy \left\{ K\left(\pi\Pi\right)^2 + \frac{1}{K}\left(\partial_y\phi\right)^2 \right\}. \qquad \text{(A5)} \end{aligned}$$

The middle term in Eq. (A5) encodes a coupling between the ϕ and Q fields, capturing the effects of the global symmetry described above. The effect of this coupling can be found explicitly by minimizing Eq. (A5) with respect to Q, subject to the boundary condition $\partial_x Q(x = 0^-, y) = 0$, which again is appropriate for an open boundary. This minimum $\Phi(x, y)$ obeys the equation

$$-\rho\nabla^2\Phi + \Delta\Phi + \sqrt{2}g\phi(y)\delta(x) = 0\,.$$

Fourier transforming with respect to y, the solution to this equation for $x \geq 0$ is

$$\Phi(x, q_y) = -\frac{\sqrt{2}g}{\rho}\frac{\phi(q_y)}{\sqrt{\Delta + \rho q_y^2}} e^{-\sqrt{(\Delta+\rho q_y^2)/\rho}\, x}.$$

We can finally write $Q = \Phi + q$, with $[p(\mathbf{r}_1), q(\mathbf{r}_2)] = i\delta(\mathbf{r}_1 - \mathbf{r}_2)$ to fully decouple the edge mode from the bulk. After some algebra, we arrive at the effective Hamiltonian at the quadratic level in the form

$$\begin{aligned} H_{eff} &\approx \int_{x\geq 0} d^2 r \left\{ \frac{1}{2}\rho\left(|\vec{\nabla}p|^2 + |\vec{\nabla}q|^2 \right) + \frac{1}{2}\Delta\left(p^2 + q^2\right) \right\} \\ &+ \frac{u}{2\pi}\int dy \left\{ K\left(\pi\Pi\right)^2 + \frac{1}{K}\left(\partial_y\phi\right)^2 \right\} \\ &+ L_y \frac{g^2}{\sqrt{\rho\Delta}}\int \frac{dq_y}{2\pi}\left[1 - \frac{1}{\sqrt{1 + \rho q_y^2/\Delta}} \right]\phi(-q_y)\phi(q_y). \qquad \text{(A6)} \end{aligned}$$

For small enough q_y, it is apparent that the last two terms of Eq. (A6) support a linearly dispersing normal mode, whose dynamics is described by a Luttinger liquid Hamiltonian with renormalized parameters. In particular, the renormalized coefficient of the $(\partial_y\phi)^2$ term is $u/K + 2\pi g^2\sqrt{\rho}/\Delta^{3/2}$. Our goal is to match the Hamiltonian controlling this mode as Δ becomes small to the result [Eq. (3.17)] of the model described in Section III, in which non-Gaussian properties of the bulk system were retained. This leads to two requirements: (*i*) The coefficient of the $(\partial_y\phi)^2$ should remain finite and non-vanishing in the limit of small Δ; (*ii*) the velocity of the gapless mode should vanish as $\Delta^{1/4}$. The first condition will be met if we assume $g \sim \Delta^{3/4}$ and $u \sim K$. Noting further that the product uK [the coefficient of the $(\pi\Pi)^2$ in Eq.

(A6)] is not renormalized, requirement (*ii*) on the velocity implies that our "bare" parameters u and K scale as $u \sim K \sim \Delta^{1/4}$, in accordance with the scaling of the normal mode parameters u_{NM}, K_{NM} derived in Section III.

Appendix B: Derivation of the general expression for δR vs. T

In this Appendix we first derive the general expression for δR [Eq. (4.23)] starting from Eq. (4.22). Inserting $\omega_{\mathbf{k}}$ from Eq. (4.19), writing the Bose function as a geometric sum and performing the integral over $\mathbf{k}$, the correlation function $\mathcal{C}(t)$ becomes

$$\mathcal{C}(t) = \lim_{\epsilon\to 0} (-1)^{-\frac{K}{4}} \left(\sinh\left(\frac{(t-i\epsilon)\,\pi}{\beta}\right)\right)^{-\frac{K}{2}} \times \frac{1}{4\pi\rho}\left(\sum_{n=0}^{\infty}\frac{e^{-\Delta(n\beta+it)}}{n\beta+it} + \sum_{n=1}^{\infty}\frac{e^{-\Delta(n\beta-it)}}{n\beta-it}\right). \tag{B1}$$

To proceed with the calculation of δR, we recast Eq. (4.22) as

$$\delta R \approx -\frac{\mathcal{D}}{4\pi\rho} I \quad \text{where} \quad I \equiv 4\pi\rho\Im m\left\{\int_0^\infty \mathrm{d}t\, t\mathcal{C}(t)\right\}. \tag{B2}$$

Substituting (B1) for $\mathcal{C}(t)$, we get

$$\begin{aligned} I &= \Im m\left\{\int_0^\infty \mathrm{d}t\cdot t\,(-1)^{-\frac{K}{4}}\left(\sinh\left(\frac{t\pi}{\beta}\right)\right)^{-\frac{K}{2}}\left(\sum_{n=0}^{\infty}\frac{e^{-\Delta(n\beta+it)}}{n\beta+it}+\sum_{n=1}^{\infty}\frac{e^{-\Delta(n\beta-it)}}{n\beta-it}\right)\right\} \\ &= \Im m\left\{\int_0^\infty \mathrm{d}t\cdot t\,(-1)^{-\frac{K}{4}}\left(\sinh\left(\frac{t\pi}{\beta}\right)\right)^{-\frac{K}{2}}\int_\Delta^\infty \mathrm{d}\Delta'\left(\sum_{n=0}^{\infty}e^{-\Delta'(n\beta+it)}+\sum_{n=1}^{\infty}e^{-\Delta'(n\beta-it)}\right)\right\} \\ &= -\int_\Delta^\infty \mathrm{d}\Delta'\sum_{n=0}^{\infty}e^{-\Delta' n\beta}\frac{\partial F_-(\Delta')}{\partial\Delta'} + \int_\Delta^\infty \mathrm{d}\Delta'\sum_{n=1}^{\infty}e^{-\Delta' n\beta}\frac{\partial F_+(\Delta')}{\partial\Delta'}, \end{aligned} \tag{B3}$$

where

$$\begin{aligned} F_\mp(\Delta) &\equiv \Im m\left\{\frac{(-1)^{-\frac{K}{4}}}{i}\int_0^\infty \mathrm{d}t\cdot e^{\mp i\Delta t}\left(\sinh\left(\frac{\pi}{\beta}t\right)\right)^{-\frac{K}{2}}\right\} = 2^{\frac{K}{2}}\frac{\beta}{2\pi}\Im m\left\{\frac{(-1)^{-\frac{K}{4}}}{i}B\left(i\gamma\pm\tfrac{K}{4},\ 1-\tfrac{K}{2}\right)\right\} \\ &= -2^{\frac{K}{2}}\frac{\beta}{2\pi}\Re e\left\{\Gamma\left(1-\frac{K}{2}\right)\left|\Gamma\left(\frac{K}{4}+i\gamma\right)\right|^2\frac{\left(\cos\pi\frac{K}{4}-i\sin\pi\frac{K}{4}\right)}{\pi}\left(\cosh\pi\gamma\sin\frac{\pi K}{2}\mp i\sinh\pi\gamma\cos\frac{\pi K}{2}\right)\right\} \\ &= -2^{\frac{K}{2}}\frac{\beta}{2\pi}\Gamma\left(1-\frac{K}{2}\right)\left|\Gamma\left(\frac{K}{4}+i\gamma\right)\right|^2\frac{1}{\pi}e^{\mp\pi\gamma}\frac{1}{2}\sin\frac{\pi K}{2}; \end{aligned} \tag{B4}$$

here $\gamma = \frac{\beta\Delta}{2\pi}$, $B(x,y) = \frac{\Gamma(x)\Gamma(y)}{\Gamma(x+y)}$ is the Beta function and we have used the identity $\Gamma(z)\Gamma(1-z) = \pi/\sin(\pi z)$. Inserting these expressions for F_+ and F_- in Eq. (B3) yields

$$\begin{aligned} I = 2^{\frac{K}{2}}\frac{\beta}{2\pi}\Gamma\left(1-\frac{K}{2}\right)\frac{1}{2\pi}\sin\frac{\pi K}{2}\times \\ \left\{-\int_\Delta^\infty \mathrm{d}\Delta'\frac{1}{1-e^{-\Delta'\beta}}\frac{\partial}{\partial\Delta'}\left(\left|\Gamma\left(\frac{K}{4}+i\gamma'\right)\right|^2 e^{-\frac{\beta\Delta'}{2}}\right)\right. \\ \left.+\int_\Delta^\infty \mathrm{d}\Delta'\frac{e^{-\Delta'\beta}}{1-e^{-\Delta'\beta}}\frac{\partial}{\partial\Delta'}\left(\left|\Gamma\left(\frac{K}{4}+i\gamma'\right)\right|^2 e^{\frac{\beta\Delta'}{2}}\right)\right\}. \end{aligned} \tag{B5}$$

Finally, after integration by parts we obtain the expression of Eq. (4.23).

The asymptotic form of $f(z)$, which dominates the limit $T \ll \Delta$ (namely, $z \to \infty$), is now obtained from Eq. (4.23) by substituting the asymptotic form of $\Gamma(z)$ at large arguments:

$$f(z) \approx (2\pi)^{2-\frac{K}{2}} \int_z^\infty \mathrm{d}x\, x^{\frac{K}{2}-1} e^{-x} \,. \tag{B6}$$

It is therefore proportional to the incomplete Gamma function $\Gamma(\frac{K}{2}, z)$, which can be further approximated for $z \to \infty$ to give

$$f\,(z) \approx (2\pi)^{2-\frac{K}{2}}\, z^{\frac{K}{2}-1} e^{-z} \,. \tag{B7}$$

This leads to the approximate expression for δR in Eq. (4.25).

[1] Y. Zhang, Z. Jiang, J. P. Small, M. S. Purewal, Y.-W. Tan, M. Fazlollahi, J. D. Chudow, J. A. Jaszczak, H. L. Stormer, and P. Kim, Phys. Rev. Lett. **96**, 136806 (2006).

[2] J. Alicea and M. P. A. Fisher, Phys. Rev. B. **74**, 075422 (2006).

[3] M. O. Goerbig, R. Moessner, and B. Doucot, Phys. Rev. B **74**, 161407 (2006).

[4] V. P. Gusynin, V. A. Miransky, S. G. Sharapov, and I. Shovkovy, Phys. Rev. B **74**, 195429 (2006).

[5] K. Nomura and A. H. MacDonald, Phys. Rev. Lett. **96**, 256602 (2006).

[6] Z. Jiang, Y. Zhang, H. L. Stormer, and P. Kim, Phys. Rev. Lett. **99**, 106802 (2007).

[7] I. F. Herbut, Phys. Rev. B. **75**, 165411 (2007)

[8] J. N. Fuchs and P. Lederer, Phys. Rev. Lett. **98**, 016803 (2007).

[9] D. A. Abanin, K. S. Novoselov, U. Zeitler, P. A. Lee, A. K. Geim and L. S. Levitov, Phys. Rev. Lett. **98**, 196806 (2007).

[10] J. G. Checkelsky, L. Li and N. P. Ong, Phys. Rev. Lett. **100**, 206801 (2008); J. G. Checkelsky, L. Li and N. P. Ong, Phys. Rev. B **79**, 115434 (2009).

[11] Xu Du, I. Skachko, F. Duerr, A. Luican, and E. Y. Andrei, Nature **462**, 192 (2009).

[12] M. O. Goerbig, Rev. Mod. Phys. **83**, 1193 (2011).

[13] A. F. Young, C. R. Dean, L. Wang, H. Ren, P. Cadden-Zimansky, K. Watanabe, T. Taniguchi, J. Hone, K. L. Shepard and P. Kim, Nat. Phys. **8**, 550 (2012).

[14] G. L. Yu, R. Jalil, B. Belle, A. S. Mayorov, P. Blake, F. Schedin, S. V. Morozov, L. A. Ponomarenko, F. Chiappini, S. Wiedmann, U. Zeitler, M. I. Katsnelson, A. K. Geim, K. S. Novoselov and D. C. Elias, PNAS **110**, 3282 (2013).

[15] D. A. Abanin, P. A. Lee, and L. S. Levitov, Phys. Rev. Lett. **96**, 176803 (2006).

[16] C. L. Kane and E. J. Mele, Phys. Rev. Lett. **95**, 146802 (2005); C.L. Kane and E.J. Mele, Phys. Rev. Lett. **95**, 226801 (2005).

[17] M. Z. Hasan and C. L. Kane, Rev. Mod. Phys. **82**, 3045 (2010); X.-L. Qi and S.-C. Zhang, Rev. Mod. Phys. **83**, 1057 (2011).

[18] H. A. Fertig and L. Brey, Phys. Rev. Lett. **97**, 116805 (2006).

[19] E. Shimshoni, H. A. Fertig and G. V. Pai, Phys. Rev. Lett. **102**, 206408 (2009).

[20] M. Killi, T.-C. Wei, I. Affleck and A. Paramekanti, Phys. Rev. Lett. **104**, 216406 (2010); S. Wu, M. Killi and A. Paramekanti, Phys. Rev. B **85**, 195404 (2012).

[21] K. Dhochak, E. Shimshoni and E. Berg, Phys. Rev. B **91**, 165107 (2015).

[22] I.F. Herbut, Phys. Rev. B **76**, 085432 (2007).

[23] J. Jung and A.H. MacDonald, Phys. Rev. B **80**, 235417 (2009).

[24] R. Nandkishore and L. S. Levitov, Phys. Scr. **T146**, 014011 (2009); R. Nandkishore and L. S. Levitov, arXiv:1002.1966.

[25] M. Kharitonov, Phys. Rev. B **85**, 155439 (2012).

[26] M. Kharitonov, Phys. Rev. B **86**, 075450 (2012).

[27] F. Wu, I. Sodemann, Y. Araki, A. H. MacDonald and T. Jolicoeur, Phys. Rev. B **90**, 235432 (2014).

[28] Bitan Roy, M.P. Kennett, and S. Das Sarma, Phys. Rev. B **90**, 201409(R) (2014).

[29] J.L. Lado and J. Fernandez-Rossier, Phys. Rev. B **90**, 165429 (2014).

[30] Y. Zhang, Z. Jiang, J. P. Small, M. S. Purewal, Y.-W. Tan, M. Fazlollahi, J. D. Chudow, J. A. Jaszczak, H. L. Stormer and P. Kim, Phys. Rev. Lett. **96**, 136806 (2006); Y. Zhao, P. Cadden-Zimansky, F. Ghahari and P. Kim, Phys. Rev. Lett. **108**, 106804 (2012).

[31] An analogous transition has been proposed for quantum Hall bilayer systems at filling factor $\nu = 2$. See, for example, S. Das Sarma, Subir Sachdev, and Lian Zheng, Phys. Rev. Lett. **79**, 917 (1997); L. Brey, Phys. Rev. Lett. **81**, 4692 (1998); J. Schliemann and A.H. MacDonald, Phys. Rev. Lett. **84**, 4437 (2000).

[32] A. F. Young, J. D. Sanchez-Yamagishi, B. Hunt, S. H. Choi, K. Watanabe, T. Taniguchi, R. C. Ashoori, P. Jarillo-Herrero, Nature **505**, 528 (2014).

[33] A similar behavior has been detected in bilayer graphene: P. Maher, C. R. Dean, A. F. Young, T. Taniguchi, K. Watanabe, K. L. Shepard, J. Hone and P. Kim, Nature Physics **9**, 154 (2013).

[34] G. Murthy, E. Shimshoni and H. A. Fertig, Phys. Rev. B **90**, 241410(R) (2014).

[35] G. Murthy, E. Shimshoni and H. A. Fertig, arXiv:1510.04255.

[36] S. M. Girvin and A. H. MacDonald in *Perspectives in Quantum Hall Effects*, S. Das Sarma and A. Pinczuk, eds. (John Wiley & Sons, 1997); D.H. Lee and C.L. Kane, Phys. Rev. Lett. **64**, 1313 (1990); S.L. Sondhi, A.Karlhede, S.A. Kivelson and E. H. Rezayi, Phys. Rev. B **47**, 16419 (1993); K. Moon, H. Mori, K. Yang, S. M. Girvin, A. H. MacDonald, L. Zheng, D. Yoshioka and S.-C. Zhang, Phys. Rev. B **51**, 5138 (1995).

[37] H.A. Fertig, L Brey, R. Côté, A.H. MacDonald, Phys. Rev. B **50**, 11018 (1994)

[38] Kun Yang, S. Das Sarma, and A. H. MacDonald, Phys. Rev. B **74** 075423 (2006).

[39] A. Auerbach, *Interacting Electrons and Quantum Magnetism* (Springer, 1994); A. Altland and B. Simons, *Condensed Matter Field Theory*, 2nd edition (Cambridge University Press, 2010).

[40] Rajaraman, *Solitons and Instantons*
[41] Ganpathy Murthy, unpublished.
[42] T. Giamarchi, *Quantum Physics in One Dimension*, (Oxford, New York, 2004).
[43] T. Giamarchi and H. J. Schulz, Phys. Rev. B **37** 325 (1988).
[44] R. Zwanzig, J. Chem. Phys. **33**, 1338 (1960); H. Mori, Prog. Theor. Phys. **33**, 423 (1965); D. Forster, *Hydrodynamic fluctuations, Broken symmetry and Correlation functions*, (Benjamin, Massachusetts, 1975); W. Götze and P. Wölfle, Phys. Rev. B **6**, 1226 (1972).
[45] A. Rosch and N. Andrei, Phys. Rev. Lett. **85**, 1092 (2000).
[46] T. L. Schmidt, S. Rachel, F. von Oppen and L. I. Glazman, Phys. Rev. Lett. **108**, 156402 (2012).
[47] I. S. Gradshteyn and I.M. Ryzhik, *Tables of Integrals, Series, and Products* (Academic, New York 1965)